THERMODYNAMICS AND STRUCTURE OF THE {WATER + METHANOL} SYSTEM VIEWED FROM THREE SIMPLE ADDITIVE PAIR-WISE INTERMOLECULAR POTENTIALS BASED ON THE RIGID MOLECULE APPROXIMATION

Ana Dopazo-Paz[1], Paula Gómez-Álvarez[2] and Diego González-Salgado[3,*]

Department of Applied Physics, Faculty of Sciences, University of Vigo, As Lagoas s/n, C.P. 32004, Ourense, Spain; e-mail: [1] anadp@uvigo.es, [2] ga_paula@uvigo.es, [3] dgs@uvigo.es

Received August 7, 2009
Accepted March 16, 2010
Published online May 31, 2010

Dedicated to Professor Ivo Nezbeda on the occasion of his 65th birthday.

The ability of three additive pair-wise intermolecular potentials to reproduce both thermodynamics and structure of the {methanol + water} system is analysed in detail using Metropolis Monte Carlo simulations. The three potentials were constructed using the OPLS model for methanol and for water, in each case, were used the TIP4P, TIP4P/2005, and TIP4P/ice, respectively. For all the potentials, the Lorentz–Berthelot combining rule was considered to calculate water–methanol cross interactions. A wide set of first- and second-order excess thermodynamic derivatives and the site–site radial distribution functions were chosen for the study. The properties were obtained at room conditions over the whole composition range and were critically compared with selected experimental data. It turns out that the simulation results of the different potentials show no qualitative differences in the radial distribution functions whereas that the excess thermodynamic properties usually decreases in the sense TIP4P > TIP4P/2005 > TIP4P/ice. The best agreement with the experiments has been found for the potential that uses the TIP4P/2005 model which demonstrates that using potentials based on phase diagram calculations significantly improve the results for this mixture. However, even in this case only partial success was found. As regards thermodynamics, it has been detected problems to describe the excess compressibility and the excess molar enthalpy. As regards structure, although it predicts clustering of methanol molecules via methyl groups after mixing, it was unable to reproduce the preservation of the pure water structure in the mixture, a well-established phenomenon observed by neutron scattering experiments.

Keywords: Water; Methanol; Monte Carlo simulation; Excess properties; Radial distribution functions; Thermodynamics.

Collect. Czech. Chem. Commun. 2010, Vol. 75, No. 5, pp. 617–635

doi:10.1135/cccc2009097

The {water (w) + methanol (m)} system has found innumerable industrial uses and also has attracted to scientific community in the basic research area. Among other applications, it has been utilized as a solvent for dyes, resins, and adhesives[1], as a component in liquid extraction processes[2], in the manufacture of safety-glass[3], and as a hydrogen source in battery prototype of electric engines[4,5]. In fundamental research, it has stimulated biochemists since it is considered that complete understanding of the behavior of these mixtures can contribute to the knowledge of more complex biological systems, which are difficult to simulate[6], and also chemical physicists due to its unexpected and eccentric thermodynamic behavior[7], the microscopic origin of which continues being a matter of debate.

The excess thermodynamic quantities have been extensively and precisely determined as functions of temperature and composition[8–14]. At room conditions, the mixing process is accompanied by a decrease in entropy (excess molar entropy S^E is negative), enthalpy (excess molar enthalpy H^E is negative), and in volume (excess molar volume V^E is negative) whereas their dependences on the methanol (or water) mole fraction x_m (or x_w) take parabolic shapes. Specially relevant is the behavior of the second-order excess derivatives. The excess partial molar volume of methanol v_m^E takes negative values and the v_m^E vs x_m curve shows a characteristic minimum at low values of x_m. The excess isobaric thermal expansivity α_p^E takes also negative values whereas the α_p^E vs x_m curve is W-shaped. Finally, less singular is the behavior shown by the excess isobaric molar heat capacity C_p^E and the isothermal compressibility κ_T^E for which positive and negative values were found, respectively, with parabolic shaped curves. The microscopic origin of these anomalies was ascribed, in the course of several decades, to the theory proposed by Franks and Evans[15,16]. Its main feature is the enhancement of the water structure during the mixing process.

Since in the 1990's, the {water + methanol} system was systematically studied using neutron scattering with the isotopic substitution technique, from which the structure factors were obtained[17–24]. These measurements were usually combined with the empirical potential structure refinement (EPSR) method[17–19], which defines an intermolecular potential reproducing the structure factors and from which the radial distribution functions were calculated. Analysis of all these results showed no enhancement of the water structure occurs in the mixture in contrast to the accepted theory. The new microscopic view was based on a highly heterogeneous mixing in the whole concentration range despite the apparent miscibility of both components. Methanol molecules aggregate through their methyl groups whereas the pure water structure is preserved in the mixture. A relation between this

picture and the thermodynamic behavior (structure–property relations) has not been yet established; it was treated only marginally[24].

A useful way of studying the structure–property relations is the molecular simulation technique for which an intermolecular potential describing the thermodynamics and structure of the system is needed. In the context of the {water + methanol} system, a great variety of additive pair-wise potentials based on the rigid molecule approximation was purposed[25–36]. These models are usually constructed from two potentials of the pure fluids to describe interactions for like molecules combined with a simple mixing rule to define the cross interactions. In most cases, these models were used to analyse structural features of this system and only in a few cases thermodynamics was included in the analysis; specifically, the thermodynamic properties involved were the first-order excess derivatives whereas that the second-order ones, more sensitive to structural features[37], were not considered (recently the v_m^E was simulated[34,38]). Although there is a lack of a complete study of structure and thermodynamics of this system, results for the analysed properties have shown that the agreement with the experiments for this type of potentials is only partial. Some authors have proposed improved potentials including flexibility[39–47] or polarizability[38,48,49], however, till this moment, the problem continues unsolved and an intermolecular potential describing both qualities is not available yet.

Although flexibility and polarizability are fully justified and their introduction will probably improve the results[38], in our opinion, the top of the additive pair-wise potentials based on the rigid molecule approximation was not reached yet. In the preceding papers, all the potentials for the pure fluids were empirical potentials whose parameters were fitted to experimental thermodynamic properties at room conditions (mainly density and vaporization enthalpy). These potentials are nowadays being substituted for a new class of improved potentials constructed by forcing their parameters to reproduce a greater amount of thermodynamic properties. The effectiveness of this procedure is particularly true for those constructed to reproduce the complete phase diagram including solid–solid, solid–liquid, and liquid–vapor equilibria. The main exponent of this idea is the TIP4P/2005 model for water[50] (the improvement of the old TIP4P model[51]) which is nowadays the best model for water being able to predict great number of its anomalies[52]. Thus, based on theses previous results, it is our opinion that intermolecular potentials constructed in such way will allow to get the top of the potentials based on the rigid molecular approximation for the description of the {water + methanol} system.

In this work, the effect of this idea has been analysed by comparing the experimental both structural and thermodynamic features of this system with the simulation results obtained from the next two intermolecular potentials: the OPLS-TIP4P+LB constructed from the OPLS model[53] for methanol and the TIP4P model[51] for water and the OPLS-TIP4P/2005+LB constructed from the OPLS model for methanol and the TIP4P/2005 model[50] for water (in both cases, the Lorentz–Berthelot (LB) combination rules were used for the calculation of cross interactions). The first potential is based on two pure fluid potentials which were obtained forcing their parameters to reproduce thermodynamic properties at room conditions. The second potential is almost equal to the first one, however, in this case the TIP4P model is substituted for the TIP4P/2005 which belongs to the new class of potentials based on phase diagram calculations. Thus, the effect of the improvement in the water potential could be analysed in an easy way. Unfortunately, till this moment there is no potential constructed for methanol using global phase diagram calculations and so the effect due to an improved potential for methanol had to be left for a future work. The OPLS model for methanol was chosen since, within the potentials fitted to thermodynamic properties at room conditions, it was found as rather reliable to be used for simulations of the {water + methanol} system[34]. Simulations were carried out at room conditions, from which radial distribution functions and a wide set of excess thermodynamic properties were calculated for the analysis. In addition, results for the third potential, the OPLS-TIP4P/ice+LB, which is similar to the previous ones but using the TIP4P/ice model for water[54], were also included which will allow us to analyse also the effect of the molecular parameters of the water molecule in the results.

METHODOLOGY

Models and Simulation Details

The TIP4P-type models[50,51,54] for water consist of four sites placed on the oxygen atom (O_w), on two hydrogen atoms (H_w, H_w), and along the H_w–O_w–H_w bisector (M-site). The OPLS model for methanol[53] consists of three sites, one of them placed on the CH_3 group (C_m) and the other two placed on oxygen (O_m) and on the hydrogen of the hydroxyl group (H_m). The molecular geometry (bond lengths and angles) as well as the values of the Lennard–Jones (LJ) parameters, ε and σ, and the charges q of the sites are given in Table I. For these models, the intermolecular interactions be-

tween sites, a and b, of the like molecules are described by the site–site potential defined as follows:

$$u_{ab} = 4\varepsilon_{ab}\left[\left(\frac{\sigma_{ab}}{r_{ab}}\right)^{12} - \left(\frac{\sigma_{ab}}{r_{ab}}\right)^{6}\right] + \frac{q_a q_a}{r_{ab}} \qquad (1)$$

where r_{ab} is the site–site separation and σ_{ab} and ε_{ab} are the LJ cross parameters computed from σ_a, σ_b and ε_a, ε_b, respectively, using the geometrical mean as imposed by the TIP4P-type models and the OPLS model. The intermolecular interactions between sites of unlike molecules (water–methanol interactions) are calculated by the same site–site potential (*1*), evaluating

TABLE I
Lennard–Jones parameters ε_a and σ_a, partial charges q_a, and geometries of the used potential models

Site a	ε_a/k_B, K	σ_a, Å	q_a, e	Geometry
OPLS methanol[53]				
O_m	85.546821	3.070	–0.700	O_m–H_m: 0.945 Å
H_m	0.0	0.0	0.435	C_m–O_m: 1.430 Å
C_m	104.16583	3.775	0.265	C_m–O_m–H_m: 108.5°
TIP4P water[51]				
O_w	78.08	3.1535	0.0	O_w–H_w: 0.9572 Å
H_w	0.0	0.0	0.52	O_w–M: 0.15 Å[a]
M	0.0	0.0	–1.04	H_w–O_w–H_w: 104.5°
TIP4P/2005 water[50]				
O_w	93.20	3.1589	0.0	O_w–H_w: 0.9572 Å
H_w	0.0	0.0	0.5564	O_w–M: 0.1546 Å[a]
M	0.0	0.0	–1.1128	H_w–O_w–H_w: 104.52°
TIP4P/Ice water[54]				
O_w	106.1	3.1668	0.0	O_w–H_w: 0.9572 Å
H_w	0.0	0.0	0.5897	O_w–M: 0.1577 Å[a]
M	0.0	0.0	–1.1794	H_w–O_w–H_w: 104.5°

[a] Along the H_w–O_w–H_w bisector.

the LJ cross parameters using the Lorentz–Berthelot mixing rule (arithmetic and geometric means for the σ_{ab} and ε_{ab}, respectively).

Monte Carlo simulations were carried out in the *NVT* and *NPT* ensembles at temperature T = 298.15 K. In all the cases, a box with N = 500 water and methanol molecules with cubic periodic boundary conditions and minimum image convention[55,56] was used, setting a cutoff distance at half of the box length. The long-range corrections were estimated by the usual LJ long-range corrections[55] for the van der Waals interactions and by the reaction field method[55,57] for the electrostatic interactions. One move to generate a new configuration involves picking randomly a molecule, translating it in all the three Cartesian directions or rotating it about one randomly chosen axis. For the *NPT* simulations, random box volume changes also generate a new possible configuration. Simulations were organized in cycles of N movements, chosen with a fixed probability of $n_{T+R}:n_V = N/1$, where n_V is the number of volume changes per cycle and n_{T+R} is the number of translational and rotational movements per cycle for which the same probability was chosen. Acceptance ratios were set to 30% for all the moves.

More specifically, thermodynamic properties for the {water+methanol} system were obtained from *NPT* simulations at pressure P = 1 atm and for 20 different compositions. These simulations were started from the last configuration obtained in previous *NVT* runs, the density of which was set to $\rho = x_m\rho_m + x_w\rho_w$, where ρ_m and ρ_w denote the experimental densities[58] at room conditions for methanol and water, respectively. The equilibration phase consisted in all the cases of 207 120 cycles and the production run consisted of 5 242 880 cycles, taking 1 048 576 configurations (one for every 5 cycles) to compute averages. The calculated properties were the mean molar potential energy U, the mean molar volume V, the mean molar configurational enthalpy H^c, the mean of the product of the molar configurational enthalpy and molar volume VH^c, the mean of the product of the molar configurational enthalpy and molar potential energy UH^c, and the mean of the square molar volume VV. The block method[56,59,60] was used to estimate the statistical errors.

On the other hand, radial distribution functions (RDFs) were evaluated for three different mixtures and for the pure fluids using simulations in the *NVT* ensemble. The chosen methanol mole fractions were 0.05, 0.27 and 0.7, the same values as those considered in the neutron scattering experiments[21–23]. The density of these simulations was obtained by interpolation at specific mole fractions of the density data obtained in the *NPT* runs. In this case, the equilibrium phase involved 100 000 cycles while the production run consisted of 750 000 cycles. 150 000 configurations (one for

every 5 cycles) were taken to determine RDFs using conventional procedures[55].

Calculation of Derived Thermodynamic Properties

The isobaric thermal expansivity α_p, the isothermal compressibility κ_T, and the residual isobaric molar heat capacity C_p^{res} were calculated from the fluctuation method[61,62] using the following relationships:

$$\alpha_p = \frac{1}{V k_\mathrm{B} T^2}(VH^\mathrm{c} - V \cdot H^\mathrm{c}) \tag{2}$$

$$\kappa_T = \frac{1}{V k_\mathrm{B} T}(VV - V \cdot V) \tag{3}$$

$$C_p^{\mathrm{res}} = \frac{1}{k_\mathrm{B} T^2}(UH^\mathrm{c} - U \cdot H^\mathrm{c}) + \frac{P}{k_\mathrm{B} T^2}(VH^\mathrm{c} - V \cdot H^\mathrm{c}) \tag{4}$$

where k_B is the Boltzmann constant. The excess properties for each mixture were obtained in the context of the Benson and Kiyohara criterion[10] as follows:

$$V^\mathrm{E} = V - x_\mathrm{m} V_\mathrm{m} - x_\mathrm{w} V_\mathrm{w} \tag{5}$$

$$H^\mathrm{E} = H^\mathrm{c} - x_\mathrm{m} H_\mathrm{m}^\mathrm{c} - x_\mathrm{w} H_\mathrm{w}^\mathrm{c} \tag{6}$$

$$C_p^\mathrm{E} = C_p^{\mathrm{res}} - x_\mathrm{m} C_{p,\mathrm{m}}^{\mathrm{res}} - x_\mathrm{w} C_{p,\mathrm{w}}^{\mathrm{res}} \tag{7}$$

$$\alpha_p^\mathrm{E} = \alpha_p - \phi_\mathrm{m} \alpha_{p,\mathrm{m}} - \phi_\mathrm{w} \alpha_{p,\mathrm{w}} \tag{8}$$

$$\kappa_T^\mathrm{E} = \kappa_T - \phi_\mathrm{m} \kappa_{T,\mathrm{m}} - \phi_\mathrm{w} \kappa_{T,\mathrm{w}} \tag{9}$$

where subscripts m and w denote methanol and water, respectively, and ϕ_m and ϕ_w are the volume fractions of methanol and water, respectively, defined as

$$\phi_m = \frac{x_m V_m}{x_m V_m + x_w V_w} \quad (10)$$

$$\phi_w = \frac{x_w V_w}{x_m V_m + x_w V_w} . \quad (11)$$

Finally, the excess partial molar volume v_m^E was calculated using its relation to the excess molar volume in the following way:

$$v_m^E = V^E + x_w \left(\frac{\partial V^E}{\partial x_w} \right)_{T,P} . \quad (12)$$

Specifically, derivation in Eq. (*12*) was done from an incremental method instead of using a fit of the excess volume values in order to avoid that the results are affected by the fitting equation. Errors in all these excess quantities were evaluated using the usual error propagation technique[63] from that of the input quantities.

RESULTS AND DISCUSSION

Excess Thermodynamic Properties

The excess molar volume V^E, the excess molar enthalpy H^E, the excess isothermal compressibility κ_T^E, and the excess partial molar volume of methanol v_m^E obtained in this work are plotted in Figs 1 and 2 as a function of composition and compared with the experimental values taken from refs[10,11,14]. As it can be seen, the three models reproduce the sign of these magnitudes. From the physical point of view, this fact means that the models predict a more packed and less compressible mixture than the corresponding pure fluids ($V^E < 0$ and $\kappa_T^E < 0$), a lower volume of methanol in mixture than in the pure fluid ($v_m^E < 0$) and a decrease in energy during mixing ($H^E < 0$). As it can be observed in Table I, the difference between the intermolecular potentials appears in the charge of the water model, which increases in the sense TIP4P < TIP4P/2005 < TIP4P/ice (this result also in an increase in both the dipolar and quadrupolar moment[64]). As it can be seen in the figures, the increase of the charge in the water molecule decreases the values of these excess properties enhancing the just commented effects. On the other hand, the shape of the curves is well reproduced for the V^E for

the three models but they are not able to predict the shift of minimum at low mole fractions of methanol of the H^E and κ_T^E curves. The shape of the v_m^E curve is predicted for the mod- els using TIP4P/2005 and TIP4P/ice. It is

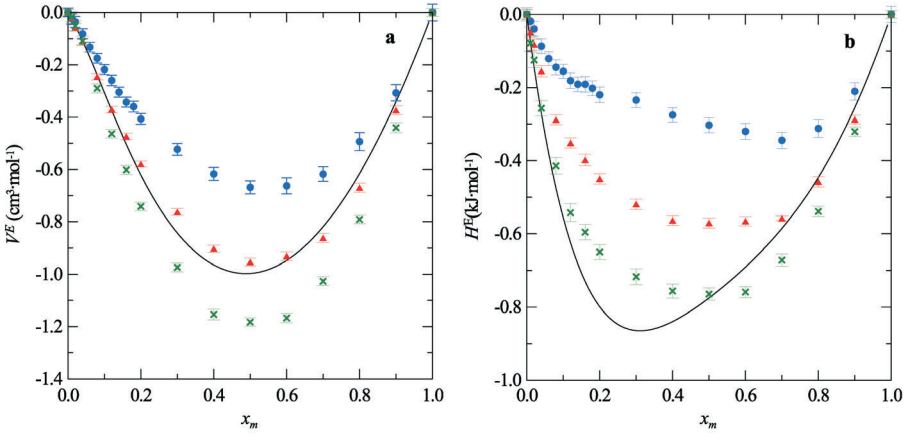

FIG. 1
Excess molar volume V^E (a) and excess molar enthalpy H^E (b) for the {water + methanol} system plotted against the methanol mole fraction x_m. OPLS+TIP4P+LB (●), OPLS+TIP4P/2005+LB (▲), OPLS+TIP4P/ice+LB (×), and experiment (full line)

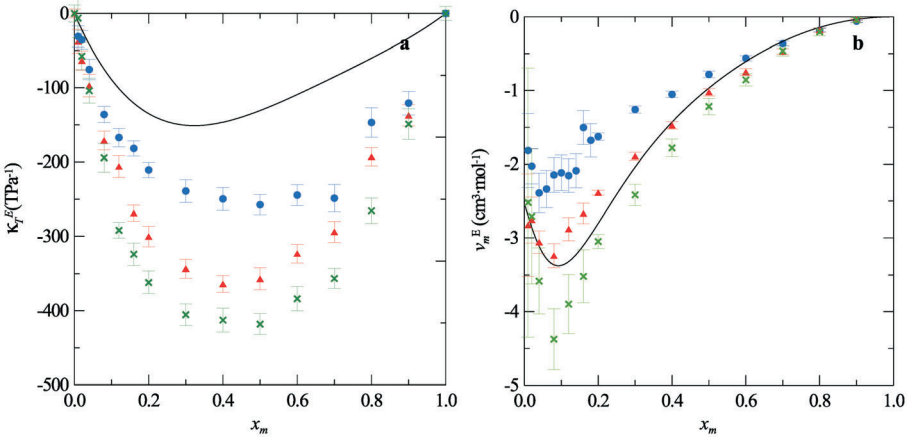

FIG. 2
Excess isothermal compressibility κ_T^E (a) and excess partial molar volume v_m^E (b) for the {water + methanol} system plotted against the methanol mole fraction x_m. OPLS+TIP4P+LB (●), OPLS+TIP4P/2005+LB (▲), OPLS+TIP4P/ice+LB (×), and experiment (full line)

worth mentioning that the minimum of the v_m^E curve is a specific characteristic of the {alcohol + water} systems[8] and these results confirm that it can be reproduced by using additive pair-wise potentials based on the rigid molecule approximation. Finally, in Fig. 3, results for the excess molar heat capacity C_p^E and the excess isobaric thermal expansivity α_p^E are given and compared to selected data from the literature[12,13]. In this case, the simulation results are slightly scattered due to a higher uncertainty usually found for the second-order magnitudes in comparison with the first-order ones. Even so, the simulation results reproduce the sign and the order of magnitude for the C_p^E; however a clear distinction between models can not be assured. As regards the α_p^E, results are not accurate enough to give any conclusion.

Overall, as it can be seen in the figures, the OPLS+TIP4P/2005+LB is the model which gives the best results for this system. This confirm our speculation that including potentials based on the phase diagram calculations significantly improve the results. In spite of this, some inefficiencies still exist: results for the excess isothermal compressibility are too low and the characteristic shape of curves of the H^E and κ_T^E is not reproduced. In the following section, the structural analysis is presented only for the OPLS+TIP4P/2005+LB model whose results were found to be similar to those obtained using the other potentials from a qualitative point of view.

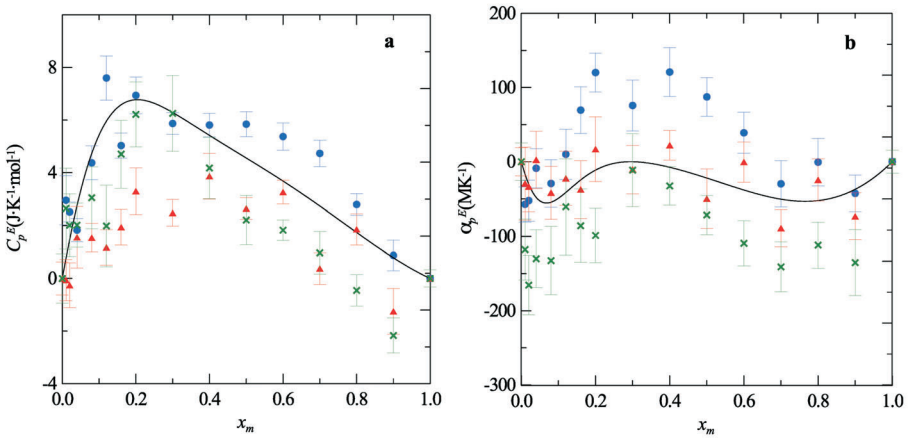

FIG. 3
Excess isobaric molar heat capacity C_p^E (a) and excess isobaric thermal expansivity α_p^E (b) for the {water + methanol} system plotted against the methanol mole fraction x_m. OPLS+TIP4P+LB (●), OPLS+TIP4P/2005+LB (▲), OPLS+TIP4P/ice+LB (×), and experiment (full line)

Radial Distribution Functions for {0.3 Water + 0.7 Methanol} Mixture

To analyse the difference between the structure of methanol and water as pure solvents and in their mixtures, Dixit et al.[23] determined, using neutron diffraction techniques and the EPSR method, a set of site–site RDFs for the {0.3 water + 0.7 methanol} mixture and the pure solvents. Among others, they evaluated the C_m–C_m and O_m–O_m RDFs for methanol and the O_w–O_w RDFs for water.

The C_m–C_m and O_m–O_m RDFs obtained from neutron scattering experiments for both pure methanol and the mixture are located at the bottom of Figs 4a and 4b, respectively. As it can be seen, when water is added to the mixture, the first peak of the C_m–C_m RDF shifts to lower radii. Likewise, the first peak of the O_m–O_m RDF decreases but does not move whereas the second peak broadens and reaches a smaller radius. Dixit et al.[23] concluded that "the addition of water has the net effect of pressing the methyl headgroups closer together while pushing the methanol hydroxyl headgroups apart, which results in a reduction of the extent of methanol–methanol hydrogen bonding in the mixture". At the top of Figs 4a and 4b, the results of our simulations for the same RDFs are shown. As it can be seen, there is a qualitative agreement between our results and the neutron scattering experiments; the first peak position for the C_m–C_m RDF of this work decreases from 4.14 Å for pure fluid to 4.03 Å for the mixture. As regards the O_m–O_m RDF, they follow the same trend as in the experiments with a reasonable quantitative agreement. Therefore, our simulation results are consistent with the conclusions of Dixit et al.[23].

The corresponding structural analysis of water can be made from Fig. 4c where similar figures to the previous ones were represented for the O_w–O_w RDF. As it can be seen at the bottom of Fig. 4c, the main experimental features after mixing are, an increase in the amplitude of the first peak keeping a similar shape and position, and the preservation of the shape, amplitude, and position (4.5 Å) of the second peak. This last characteristic is an indicator of the tetrahedral hydrogen bond network present in pure water. Hence, it is considered that the local pure water structure does not change after mixing. Simulation results, plotted at the top of Fig. 4c, show significant changes with respect to the experimental results. A remarkable increase of the first peak, much higher than the corresponding to the experimental one, and the second peak shifts to larger distances. In that sense, the results are not consistent with the invariance of the tetrahedral structure of water found by the neutron scattering experiments.

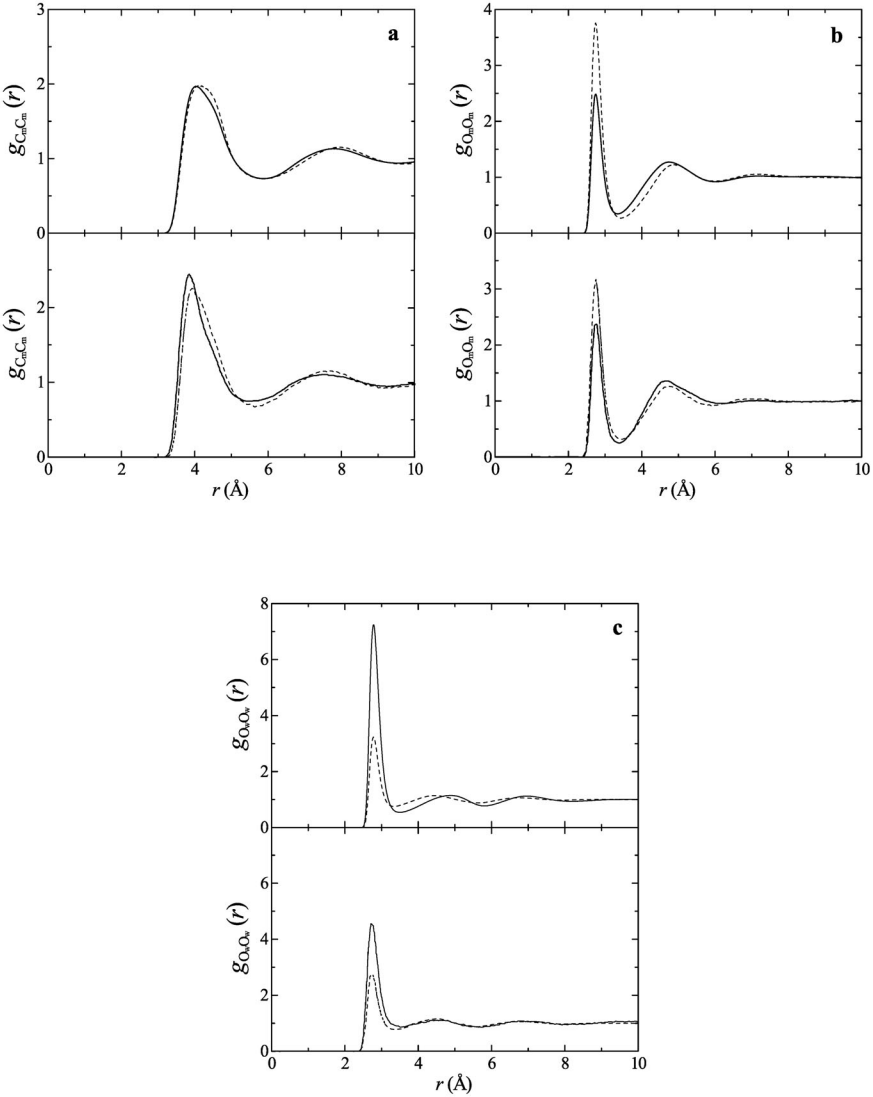

FIG. 4

Site–site radial distribution functions between C_m-sites in methanol $g_{C_mC_m}$ (a), O_m-sites in methanol $g_{O_mO_m}$ (b), and O_w-sites in water $g_{O_wO_w}$ (c). Pure fluid (dashed line) and {0.3 water + 0.7 methanol} mixture (full line). Plots at the top of each figure are simulation results and those at the bottom are data obtained from neutron scattering experiments

Radial Distribution Functions for {0.73 Water + 0.27 Methanol} Mixture

Dougan et al.[22] made a similar analysis like Dixit et al. using in this case the {0.73 water + 0.27 methanol} mixture and the C_m–C_m RDF for methanol and the O_w–O_w for water. These data plotted at the bottom of Figs 5a and 5b, are compared with those obtained in this work, which are shown at the top. As it can be seen in the experimental RDFs, the first peak of the C_m–C_m RDF shifts to lower radii and the second peak of the O_w–O_w RDF remains unchanged. These results support the structural interpretation suggested by Dixit et al.[23] in terms of a clustering of methanol molecules via methyl groups association and preservation of water structure after mixing. The behavior of the RDFs of this work (at the top of Figs 5a and 5b) is only partly in agreement with the experimental results. The shift of the first peak of the C_m–C_m RDF is reproduced; however, the position of the second peak of the O_w–O_w RDF is higher in the mixture than in pure water. This tendency is identical with that obtained for the previous mixture. Although the clustering of methanol molecules is predicted, the structure of pure water is no longer preserved.

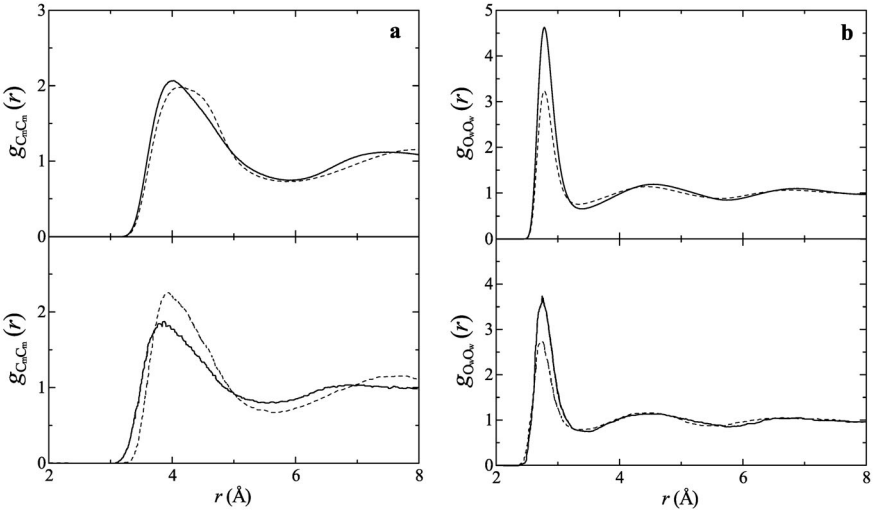

FIG. 5

Site–site radial distribution functions between C_m-sites in methanol $g_{C_mC_m}$ (a), and O_w-sites in water $g_{O_wO_w}$ (b). Pure fluid (dashed line) and {0.73 water + 0.27 methanol} mixture (full line). Plots at the top of each figure are simulation results and those at the bottom are data obtained from neutron scattering experiments

Radial Distribution Functions for {0.95 Water + 0.05 Methanol} Mixture

Dixit et al.[21] studied the variation of the structure of both water and methanol, from the pure fluid to that in the {0.95 water +0.05 methanol} mixture using C_m–C_m and O_m–O_m RDFs for methanol, and the H_w–H_w, O_w–H_w and O_w–O_w RDFs for water. These results are compared with our simulation data in Figs 6 and 7, respectively. As regards methanol, the qualitative trend found by Dixit et al.[23] based on the clustering of the methanol molecules as well as the reduction of the H-bonding of methanol molecules after mixing is also shown in the experimental RDFs (Fig. 6, bottom) and the simulated RDFs (Fig. 6, top) for this mixture. In both cases, it is clear that the position of the first peak of the C_m–C_m RDF takes a smaller value whereas that the amplitude of the second peak is reduced (to a greater extent for the results of this work). In the case of water, Fig. 7a and 7b (bottom) clearly indicate that experimental H_w–H_w and O_w–H_w RDFs are not affected by the methanol presence. This fact is also reflected by RDFs in this work (top) and supported by no perturbation scheme. However, the second peak of the O_w–O_w

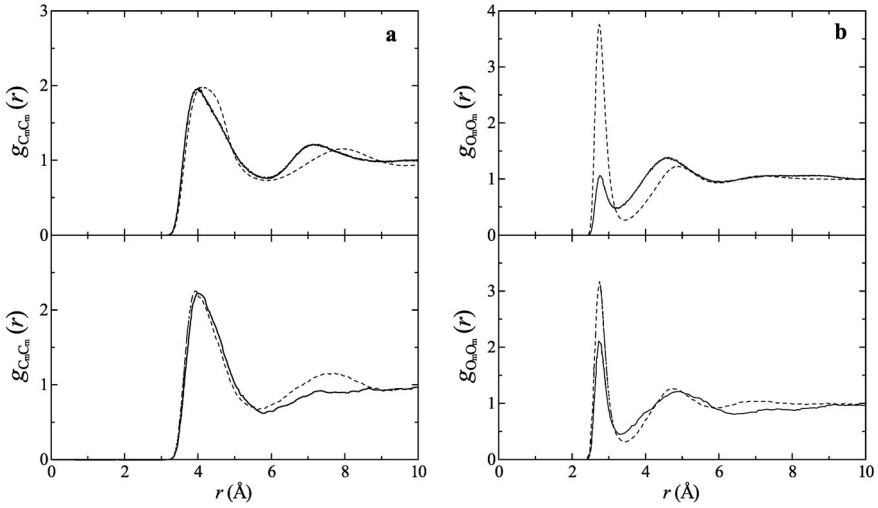

FIG. 6
Site–site radial distribution functions between C_m-sites in methanol $g_{C_mC_m}$ (a), and O_m-sites in methanol $g_{O_mO_m}$ (b). Pure fluid (dashed line) and {0.95 water + 0.05 methanol} mixture (full line). Plots at the top of each figure are simulation results and those at the bottom are data obtained from neutron scattering experiments

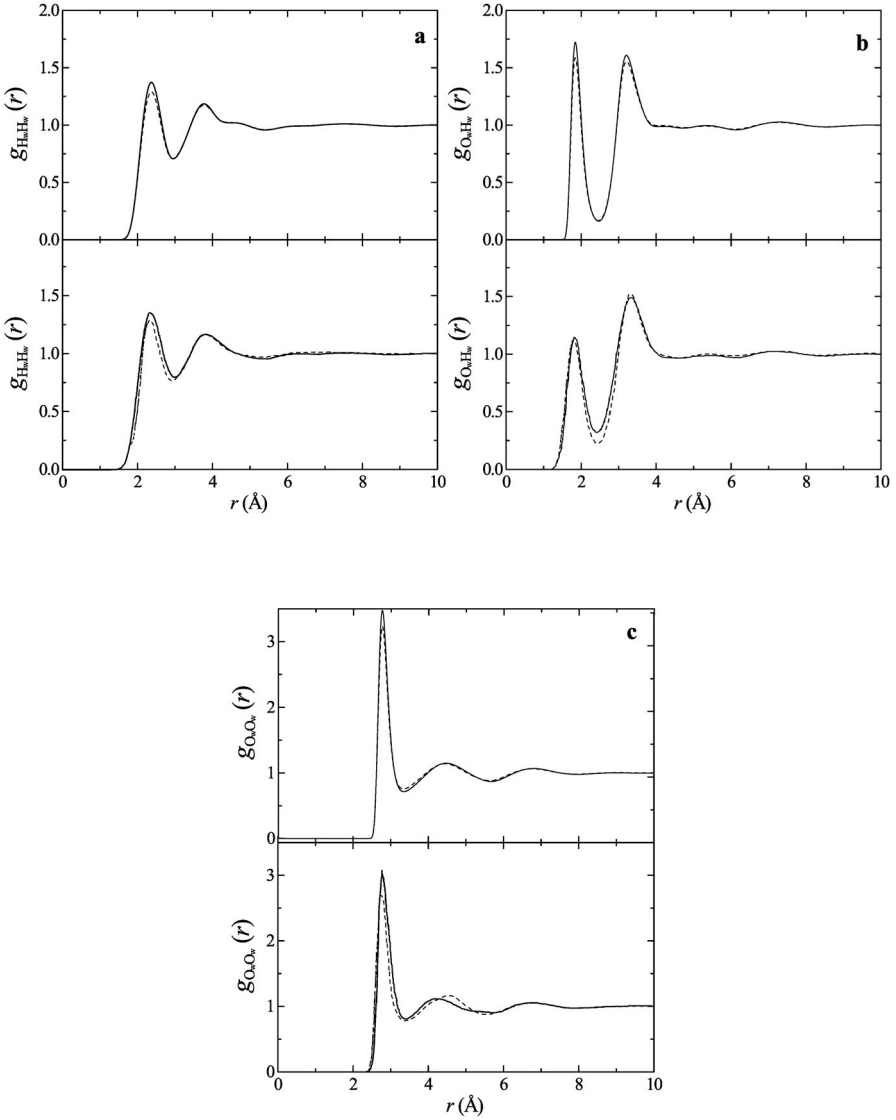

FIG. 7

Site–site radial distribution functions for water between H_W-sites $g_{H_WH_W}$ (a), O_W-site and H_W-sites $g_{O_WH_W}$ (b), and O_W-sites $g_{O_WO_W}$ (c). Pure fluid (dashed line) and {0.95 water + 0.05 methanol} mixture (full line). Plots at the top of each figure are simulation results and those at the bottom are data obtained from neutron scattering experiments

RDF obtained from scattering experiments (Fig. 7c, bottom) shifts to lower radii in the mixture relative to pure water, which suggests compression to the second-neighbor water level. This decrease in the structural freedom of water molecules is not reflected by simulation results (Fig. 7c, top) since the second peak remains in the same position.

CONCLUSIONS

The extensive simulations in this work have allowed to analyse the ability of a three additive pair-wise intermolecular potentials based on the rigid molecule approximation (OPLS+TIP4P+LB, OPLS+TIP4P/2005+LB, OPLS+TIP4P/ice+LB) to determine the thermodynamics and structure of the {water + methanol} system. The potentials differ only in the potentials for water (TIP4P, TIP4P/2005, and TIP4P/ice) which were constructed by forcing their parameters to reproduce different sets of thermodynamic properties at different temperature and pressure conditions. In a few words, the TIP4P model was obtained from thermodynamic properties of liquid at room conditions whereas that the TIP4P/2005 and TIP4P/ice are based on a new class of potentials obtained forcing them to reproduce the global phase diagram; in the TIP4P/ice attention was paid in reproducing solid features, whereas that the TIP4P/2005 was fitted to both liquid and solid properties. At a molecular lever, differences between models appear in the charge of the molecule which follow this relation TIP4P < TIP4P/2005 < TIP4P/ice. Results of this work for these three potentials have shown that the increase in the charge of the water model reduces the values of most of the excess thermodynamic properties but no qualitative differences appear in the radial distribution functions. The best agreement with the experiments has been found for the potential that uses the TIP4P/2005 model which proves that using potentials based on phase diagram calculations significantly improve the results for this mixture. However, results have shown that even this potential reflects only partly the behavior of the system. As regards thermodynamics, the main problems are the small values obtained for the κ_T^E and the erroneous shape of the curves against methanol mole fraction of the H^E and κ_T^E. As for the structure, the RDFs evaluated from this potential reflect most of the main characteristics obtained from neutron scattering experiments. Thus, the clustering of methanol molecules via methyl groups as well as the reductions in H-bond contacts of methanol molecules after mixing is adequately predicted. However, one of the main features obtained experimentally, viz. the invariance of the water structure in the mixtures relative to the pure liquid was not reflected. In summary, although

the inclusion of the TIP4P/2005 model have improved the results evidently there is room for improvement. An appealing solution is to use also for methanol an improved potential based on phase diagram calculations.

The authors are grateful to the Dirección Xeral de I + D da Xunta de Galicia (projects PGIDIT-06-PXIB-3832828-PR and INCITE08E1R383012ES) and Universidad de Vigo (project 08VI-A12) for financial support, even to the Social European Fund as well as to the Dirección Xeral de Ordenación e Calidade do Sistema Universitario de Galicia from the Consellería de Educación e Ordenación Universitaria-Xunta de Galicia for grant funding to A. Dopazo-Paz, and to the Ministerio de Educación y Ciencia under the Programa Nacional de Formación del Profesorado Universitario (No. AP-2007-2947) for supporting the research of P. Gómez-Álvarez. We also want to thank the Center of Supercomputing of Galicia for providing computing facilities.

REFERENCES

1. Primo Yúfera E.: *Química Inorgánica Básica y Aplicada: De la Molécula a la Industria*. Universidad Politécnica de Valencia, Barcelona 2003.
2. Neue U. D.: *HPLC Columns: Theory, Technology, and Practice*. Wiley-VCH, Inc., New York 1997.
3. Duffie J. A., Beckman W. A.: *Solar Engineering of Thermal Processes*. Wiley, New York 1991.
4. Tyler G.: *Environmental Science: Problems, Connections and Solutions*. Cengage Learning Eds, California 2007.
5. *Información Tecnológica*. Vol. 5, No. 2. La Serena, Chile 1994.
6. Ball P.: *Chem. Rev.* **2008**, *108*, 74.
7. Aliev M. M., Magge J. W., Abdulagatov I. M.: *Int. J. Thermophys.* **2003**, *24*, 1551.
8. Franks F., Ives D. J. G.: *Quant. Rev., Chem. Soc.* **1966**, *20*, 1.
9. Franks F., Desnoyers J. E.: *Water Sci. Rev.* **1989**, *1*, 171.
10. Benson G. C., Kiyohara O.: *J. Solution Chem.* **1980**, *9*, 791.
11. Lama R. F., Lu B. C.-Y.: *J. Chem. Eng. Data* **1965**, *10*, 216.
12. Benson G. C., D'Arcy P. J., Kiyohara O.: *J. Solution Chem.* **1980**, *9*, 931.
13. Benson G. C., D'Arcy P. J.: *J. Chem. Eng. Data* **1982**, *27*, 439.
14. Easteal A. J., Woolf L. A.: *J. Chem. Thermodyn.* **1985**, *17*, 49.
15. Frank H. S.: *J. Chem. Phys.* **1945**, *13*, 507.
16. Frank H. S., Evans M. W.: *J. Chem. Phys.* **1945**, *13*, 478.
17. Soper A. K.: *Chem. Phys.* **1996**, *202*, 295.
18. Soper A. K.: *Mol. Phys.* **2001**, *99*, 1503.
19. Bowron D. T., Finney J. L., Soper A. K.: *J. Phys. Chem. B* **1998**, *102*, 3551.
20. Soper A. K., Finney J. L.: *Phys. Rev. Lett.* **1993**, *71*, 4346.
21. Dixit S., Soper A. K., Finney J. L., Crain J.: *Europhys. Lett.* **2002**, *59*, 377.
22. Dougan L., Bates S. P., Hargreaves R., Fox J. P., Crain J., Finney J. L., Réat V., Soper A. K.: *J. Chem. Phys.* **2004**, *121*, 6456.
23. Dixit S., Crain J., Poon W. C. K., Finney J. L., Soper A. K.: *Nature* **2002**, *416*, 829.
24. Soper A. K., Dougan L., Crain J., Finney J. L.: *J. Phys. Chem.* **2006**, *110*, 3472.
25. Okazaki S., Nakanishi K., Touhara H.: *J. Chem. Phys.* **1983**, *78*, 454.
26. Okazaki S., Touhara H., Nakanishi K.: *J. Chem. Phys.* **1984**, *81*, 890.
27. Tanaka H., Gubbins K. E.: *J. Chem. Phys.* **1992**, *97*, 2626.

28. Tanaka H., Walsh J., Gubbins K. E.: *Mol. Phys.* **1992**, *76*, 1221.
29. Koh C., Tanaka H., Walsh J. M., Gubbins K. E., Zollweg J. A.: *Fluid Phase Equilib.* **1993**, 8351.
30. Freitas L. C. G.: *J. Mol. Struct.* **1993**, *282*, 151.
31. Laaksonen A., Kusalik P. G., Svishchev I. M.: *J. Phys. Chem. A* **1997**, *101*, 5910.
32. Kiselev M., Noskov S., Puhovski K., Kerdcharoen T., Hannangbua S.: *J. Mol. Graphics Modell.* **2001**, *19*, 412.
33. Nieto-Draghi C., Hargreaves R., Bates S. P.: *J. Phys.: Condens. Matter* **2005**, *17*, S3265.
34. Gonzalez-Salgado D., Nezbeda I.: *Fluid Phase Equilib.* **2006**, *240*, 161.
35. Vlček L., Nezbeda I.: *J. Mol. Liq.* **2007**, *131–132*, 158.
36. Bako I., Megyes T., Balint S., Grosz T., Chiaia V.: *Phys. Chem. Chem. Phys.* **2008**, *10*, 5004.
37. Cerdeirina C. A., Troncoso J., Gonzalez-Salgado D., Garcia-Miaja G., Hernandez-Segura G. O., Bessieres D., Medeiros M., Romani L., Costas M.: *J. Phys. Chem. B* **2007**, *111*, 1119.
38. Moučka F., Nezbeda I.: *Collect. Czech. Chem. Commun.* **2009**, *74*, 559.
39. Bolis G., Corongiu G., Clementi E.: *Chem. Phys. Lett.* **1982**, *86*, 299.
40. Jorgensen W. L., Madura J. D.: *J. Am. Chem. Soc.* **1983**, *105*, 1407.
41. Ferrario M., Haughney M., McDonald I. R., Klein M. L.: *J. Chem. Phys.* **1990**, *93*, 5156.
42. Pálinkás G., Hawlicka E., Heinzinger K.: *Chem. Phys.* **1991**, *158*, 65.
43. Pálinkás G., Bako I., Heinzinger K., Boop P.: *Mol. Phys.* **1991**, *73*, 897.
44. Noskov S. Y., Kiselev M. G., Kolker A. M., Rode B. M.: *J. Mol. Liq.* **2001**, *91*, 157.
45. Wensink E. J. W., Hoffmann A. C., van Maaren P. J., van der Spoel D.: *J. Chem. Phys.* **2003**, *119*, 7308.
46. Allison S. K., Fox J. P., Hargreaves R., Bates S. P.: *Phys. Rev. B* **2005**, *71*, 024201.
47. Dougan L., Hargreaves R., Bates S. P., Finney J. L., Reat V., Soper A. K., Crain J.: *J. Chem. Phys.* **2005**, *122*, 174514.
48. Yu H., Geerke D. P., Liu H., Van Gunsteren W. F.: *J. Comput. Chem.* **2006**, *27*, 1494.
49. Zhong Y., Lee Warren G., Patel S.: *J. Comput. Chem.* **2008**, *29*, 1142.
50. Abascal J. L. F., Vega C.: *J. Chem. Phys.* **2005**, *123*, 234505.
51. Jorgensen W. L., Chandrasekhar J., Madura J. D., Impey R. W., Klein M. L.: *J. Chem. Phys.* **1983**, *79*, 926.
52. Pi H. L., Aragonés J. L., Vega C., Noya E. G., Abascal J. L. F., González M. A., McBride C.: *Mol. Phys.* **2009**, *107*, 365.
53. Jorgensen W. L.: *J. Phys. Chem.* **1986**, *90*, 1276.
54. Abascal J. L. F., Sanz E., García Fernández R., Vega C.: *J. Chem. Phys.* **2005**, *122*, 234511.
55. Allen M. P., Tildesley D. J.: *Computer Simulation of Liquids*. Oxford University Press, Oxford 1987.
56. Frenkel D., Smit B.: *Undestanding Molecular Simulation: From Algorithms to Applications*. Academic Press, California 1996.
57. Onsager L.: *J. Am. Chem. Soc.* **1936**, *58*, 1486.
58. Riddick J. A., Bunger W. B., Sakano T.: *Organic Solvents, Physical Properties and Methods of Purification*, Vol. II. Wiley, New York 1986.
59. Flyvbjerg H., Petersen H. G.: *J. Chem. Phys.* **1989**, *91*, 461.
60. Whitmer C.: *Phys. Rev. D* **1984**, *29*, 306.
61. Lagache M., Ungerer P., Boutin A., Fuchs A. H.: *Phys. Chem. Chem. Phys.* **2001**, *3*, 4333.
62. Pineiro M. M., Cerdeirina C. A., Medeiros M.: *J. Chem. Phys.* **2008**, *129*, 014511.

63. Bevington P. R., Robinson D. K.: *Data Reduction and Error Analysis for the Physical Sciences*. McGraw–Hill, New York 1992.
64. Abascal J. L. F., Vega C.: *J. Phys. Chem.* **2007**, *111*, 15811.